INVITED PAPER

# Terahertz Spectroscopy and Imaging for Defense and Security Applications

*Laboratory experiments indicate that, with more powerful sources and more sensitive detectors, terahertz techniques have great potential for detection and identification of concealed explosives.*

By Hai-Bo Liu, *Member IEEE*, Hua Zhong, Nicholas Karpowicz, Yunqing Chen, and Xi-Cheng Zhang, *Fellow IEEE*

**ABSTRACT** | Terahertz (THz) radiation, which occupies a relatively unexplored portion of the electromagnetic spectrum between the mid-infrared and microwave bands, offers innovative sensing and imaging technologies that can provide information unavailable through conventional methods such as microwave and X-ray techniques. With the advancement of THz technologies, THz sensing and imaging will impact a broad range of interdisciplinary fields, including chemical and biological detections and identifications. In particular, THz radiation offers the opportunity for transformational advances in defense and security. Recent work shows that THz technologies are promising for the standoff detection and identification of explosive targets.

**KEYWORDS** | Submillimeter-wave generation; submillimeter-wave imaging; submillimeter-wave measurements; submillimeter-wave spectroscopy

## I. INTRODUCTION

Terahertz (THz) waves, or submillimeter/far-infrared waves, refer to electromagnetic radiation in the frequency interval from 0.1 to 10 THz. They occupy a large portion of the electromagnetic spectrum between the mid-infrared and microwave bands (in different units: 1 THz $\leftrightarrow$ 1 ps $\leftrightarrow$ 300 $\mu$m $\leftrightarrow$ 33.3 cm$^{-1}$ $\leftrightarrow$ 4.1 meV $\leftrightarrow$ 47.6 K). In comparison with relatively well-developed technologies and widespread applications in microwave, mid-infrared, and optical bands, basic research, advanced technology developments, and real-world applications in the THz band are still in infancy. During the past decade, various THz technologies have been undergoing rapid development and have enabled us to apply THz sensing and imaging for chemical, biological, biomedical and other interdisciplinary study. In recent years, THz technologies have proven to be promising methods for defense and security applications.

The spectral domain from 0.1 to 10 THz hosts low frequency crystalline lattice vibrations (phonon modes), hydrogen-bonding stretches, and other intermolecular vibrations of molecules in many chemical and biological materials, including explosives and related compounds (ERCs), drugs and other biomolecules. Many polar gases also have distinctive spectroscopic fingerprints in the THz range. The transmitted and reflected THz spectra of these materials contain THz absorption fingerprints characterizing these THz vibrational modes and provide information that is not available in other parts of the electromagnetic spectrum. THz waves have low photon energies (4 meV for 1 THz, 1 million times weaker than X-ray photons) and will not cause harmful photoionization in biological tissues [1], [2]. As a potential sensing and imaging modality, THz radiation is considered a safe method for the operators and targets. THz radiation can penetrate through many commonly used nonpolar dielectric materials, such as paper, cardboard, textile, plastic, wood, leather, and ceramic with little attenuation. Therefore, THz technologies can be used for nondestructive or noninvasive sensing and imaging of targets under

Manuscript received October 31, 2005; revised March 20, 2007. This work was supported in part by U.S. Army Research Office under the MURI under Project DAAD190210255, in part by a HSARPA SBIR grant through Intelligent Optical Systems, and in part by the National Science Foundation under CenSSIS Grant EEC-9986821 and IGERT Grant 0333314.

**H.-B. Liu** was with Center for Terahertz Research, Rensselaer Polytechnic Institute, Troy, NY 12180 USA. He is now with InterScience, Inc., Troy, NY 12180 USA (e-mail: liuh@intersci.com).

**H. Zhong**, **N. Karpowicz**, **Y. Chen**, and **X.-C. Zhang** are with Rensselaer Polytechnic Institute, Troy, NY 12180 USA (e-mail: zhangxc@rpi.edu).

Digital Object Identifier: 10.1109/JPROC.2007.898903

covers or in containers in some cases. Owing to these advantages, THz technologies have been considered competitive methods for inspecting hidden explosives, chemical/biological threats and defects for defense and security applications in the real world.

Recently THz spectroscopy and imaging of ERCs have been investigated intensively for possible defense and security applications. In 2003, Kemp *et al.* [3] reported measurements showing THz spectral features in a number of common energetic explosives, such as 2,4,6-trinitrotoluene (TNT), hexahydro-1,3,5-trinitro-1,3,5-triazine (RDX), tetramethylene tetranitramine (HMX), pentaerythritol tetranitrate (PETN), and commercial explosives like PE-4 and Semtex. Subsequently, we reported THz spectra of 14 ERCs obtained by both THz time-domain spectroscopy (THz-TDS) and Fourier-transform far-infrared spectroscopy [4]. Yamamoto *et al.* [5] and Huang *et al.* [6] reported the THz absorption of RDX validating the results of Kemp *et al.* [3]. Most of these THz absorption fingerprints below 3 THz are from the lattice vibrational modes of solid-state explosive materials. THz spectroscopy in a transmission mode was used for explosives sensing in these investigations [3]–[6]. However, for practical applications, reflection measurements are preferred since most bulky targets are impossible to be measured in a transmission mode. Furthermore, reflection spectroscopy, especially diffuse reflection spectroscopy (superior to specular reflection spectroscopy in inspecting irregular surfaces in real-world scenarios), is more applicable for standoff detection than transmission methods. Detection of RDX by THz specular reflection spectroscopy has been demonstrated recently by Shen *et al.* [7]. In our laboratory, we have investigated the THz diffuse reflection spectra of explosives using RDX as a model compound. Our results imply that THz diffuse reflection spectroscopy has a great potential for the detection and identification of explosives concealed in packages or under clothing [8]. In addition, we have successfully sensed RDX by THz specular reflection spectroscopy at a standoff distance of 30 m [9].

In addition to sensing with THz spectroscopy, 2-D and 3-D THz spectroscopic imaging are also focused interests of worldwide researchers. Detection of RDX by THz specular reflection spectroscopic imaging has been reported by Shen *et al.* [7]. In our lab, we used both pulsed THz imaging and continuous-wave (CW) THz imaging for the security scanning of packages, bags and shoes. Kawase *et al.* used THz spectroscopic imaging for drug detections in envelopes [10]. Compared with commonly used inspection techniques such as X-ray imaging, THz imaging offer advantages including spectroscopic information, nonionizing irradiation, and higher image contrast for differentiating between various soft materials. These advantages stem from the fact that THz radiation is more sensitive to the nature of these materials it passes through [10]. For instance, an air bulb or a defect in the foam can be more easily identified with THz radiation rather than X-ray in most cases.

In this paper, different THz generation and detection technologies are reviewed briefly and the propagation of THz waves in the atmosphere is described. Subsequently, we report recent THz sensing and imaging results achieved in our laboratory. Using both a THz-TDS system and a Fourier transform far-infrared spectrometer, we obtained a THz spectral database for ERCs in the range of 0.1–21 THz. Density functional theory is employed to calculate structures and vibrational modes of several important ERCs. We demonstrate the detection and identification of explosive RDX by diffusely reflected THz waves. Sensing RDX with THz specular reflection spectroscopy at a standoff distance of 30 m is also recorded. Finally we review the pulsed THz imaging with THz-TDS and describe the CW THz imaging of various targets, such as bags and shoes. Our investigations, together with other work from worldwide researchers, demonstrate that THz spectroscopy and imaging will play significant roles in the fields of defense and security.

## II. GENERATION AND DETECTION OF THz WAVES

THz waves, either broadband waves or narrow-linewidth CW, can be generated and detected by various methods. Each of them has different output power, efficiency, bandwidth, dynamic range, signal-to-noise ratio (SNR), and technological implementation.

A brief discussion of the different types of sources and detectors will assist the considerations of applying THz spectroscopy and imaging in defense and security fields.

### A. Broadband THz Systems

The broadband thermal emitters, such as glowbars and mercury lamps, and liquid-helium cooled bolometers are conventionally used in Fourier transform far-infrared spectroscopy systems. However, they are limited within laboratory investigations due to low output powers and liquid-helium cooling.

Free electron lasers are the most powerful sources of THz radiation available, producing either CW or pulsed beams of coherent THz waves with an efficiency potentially close to unity [11]. However, their bulky size and high cost prevent their use in nonlaboratory applications.

THz-TDS, or THz pulsed spectroscopy based on ultrafast lasers has been developing since the 1990s. This technology generates and detects picosecond THz pulses by a coherent and time-gated method using near-infrared femtosecond lasers. In THz-TDS, the amplitude and phase of each spectral component of the THz pulse can be determined, thereby allowing the complex dielectric properties of materials to be characterized. The generated THz power in THz-TDS is not high, with an average power from nW [12] to 650 $\mu$W [13]. However, using time-gated

lock-in detections, the achieved dynamic range of the measured THz power spectrum can reach up to 80 dB. Biased photoconductive antennas, which are made of semi-insulating GaAs [14], [15] or low-temperature-grown GaAs (LT-GaAs) [16], [17], are the early sources and detectors used in THz-TDS. Unbiased bulk semiconductors and other crystals, such as InAs, InSb [18], [19], ZnTe [20], InP, GaP, GaAs [21], GaSe [22], [23], $LiNbO_3$ [24], $LiTaO_3$ [25], and polymer films [26], [27] are also widely used as THz emitters, based upon the mechanism of either the ultrafast transport of charged carriers or the optical rectification. The bandwidth of the radiated THz spectrum depends on the laser bandwidth, the emitter and the detector. Using short laser pulses with a pulse duration of $\sim$10 fs along with specific emitters and detectors, the achieved bandwidth can reach up to 60–100 THz [25]–[30], by trading off SNR. Usually a system with a narrower bandwidth has a higher SNR. For instance, using LT-GaAs antennas as the emitter and detector, a THz spectrum with a smooth spectral distribution between 0.3 and 7.5 THz, and a dynamic range of $\sim$60 dB (for THz power) was obtained [31], which is ideal for THz spectroscopic sensing.

In THz-TDS, the coherent THz detectors include photoconductive antennas [14], [15] and nonlinear crystals based on electrooptic (EO) sampling [32], [33]. Broadband THz waves are usually detected using EO sampling [25], [26], [28], [29] and the bandwidth of detected THz spectra depends on the thickness of the crystal [34]. Any one of the mentioned emitters can combine either of the detection methods to make up a THz-TDS system with specific bandwidth, dynamic range, SNR, etc.

### B. Narrowband Continuous-Wave THz Systems

CW systems with narrowband THz radiation can be used for imaging and spectroscopy with high spectral resolution. Electronic sources include frequency-multiplied Gunn diode oscillators and backward wave oscillators (BWOs). Gunn diode oscillators can provide power ranging from $\sim$200 mW near 0.1 THz to $\sim\mu$W near 1.7 THz [35], [36]. The BWO's power varies from $\sim$100 mW at 0.1 THz to $\sim$1 mW at 1.25 THz [37], [38]. Scanning THz spectrometers based on BWOs and Golay cell detectors are commercially available, with a spectral tuning range of 35 GHz–1.25 THz, resolutions of 1–10 MHz and a dynamic range of 60 dB [37], [38]. Nonlinear optical sources include THz-wave parametric oscillators (TPOs) and photocurrent-based photomixers. TPOs provide ns THz pulses with the maximum THz peak power of above 100 mW, and a range of 0.7–3.8 THz [10], [39]. Photocurrent-based photomixers using biased semiconductors with ultrafast carrier recombination time have a tuning range from 0.1 to above 3 THz in a single device, with power levels typically below 1 $\mu$W beyond 1 THz [40]–[43]. There are also three types of THz lasers available for CW generation: gas lasers, quantum cascade lasers (QCLs), and free-electron lasers (FELs). THz gas lasers are not continuously tunable, but have been shown to operate at over 2000 frequencies from 0.9 to 6.86 THz, with power levels ranging from 1 to $\sim$180 mW [44]. The QCL is a major step toward a compact and practical electrically pumped THz emitter. It features high output powers (above 100 mW) and a control of layer thickness which allows the emission wavelength to be designed in (the lowest frequency reaches $\sim$2.1 THz) [45]–[47]. However, it works at liquid-helium or liquid-nitrogen temperature. FELs are very powerful pulsed or CW sources for widely tunable and coherent radiation. But their large sizes limit their applications.

CW detectors can be either narrowband or broadband. Schottky diodes are fairly compact but lacking in frequency agility, and their cost is very high beyond 1 THz [48], [49]. Broadband detectors include bolometers, Golay cells and pyroelectric detectors. Liquid-helium cooled bolometers are broadband and sensitive THz wave detectors with fast response, but they are difficult to implement in real fields because they use liquid-helium. Compact sources Golay cells can detect a frequency range of 0.02–20 THz with a high dynamic range of 50 dB. But they have a long response time (a few tens of ms), and the maximum input power is limited to a few tens of $\mu$W [50]. Pyroelectric detectors cover a spectral range from 0.1 to beyond 20 THz with $\sim$ms response time, and compact units are also available [51]. In addition, heterodyne detection methods can achieve very low detection limits, which are several orders lower than that of the direct detection methods.

### C. Compact THz Systems

For the purpose of applications outside of laboratory settings, compact or portable THz systems with the similar capabilities as robust systems are desirable. In our lab, both compact broadband THz systems and portable CW narrow-linewidth systems have been developed. The broadband THz system is a portable THz-TDS setup powered by an IMRA femtosecond fiber laser, with a size of 55 cm $\times$ 40 cm $\times$ 20 cm and a weight of $\sim$22 lb, as shown in Fig. 1(a). It provides real-time spectroscopy measurements at rates up to 4 Hz with a dynamic range (THz amplitude) of $\sim$100 in the 0.1–2 THz range. The narrow-linewidth CW systems shown in Fig. 1(b) are smaller (25 cm $\times$ 20 cm $\times$ 13 cm), consisting of Gunn diodes sources (100–800 GHz) and Schottky diodes or pyroelectric detectors. The 0.2 and 0.4 THz systems weigh 9 lb and 6 lb respectively. They provide measurements with a dynamic range of 25–40 dB and a line scan speed up to 0.6 m/s. Other portable narrow-linewidth and broadband THz-wave parametric generators were also reported [52].

## III. PROPAGATION OF THz WAVES IN THE ATMOSPHERE

One of the major hurdles for THz free-space sensing and imaging is the atmospheric attenuation dominated by

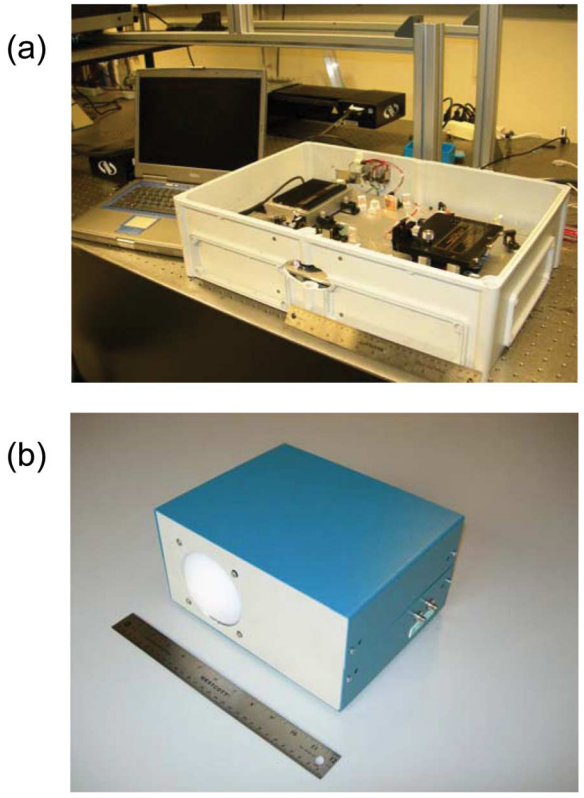


**Fig. 1.** *(a) Compact broadband THz-TDS system, with a size of 55 cm × 40 cm × 20 cm and a weight of ~22 lb. (b) CW narrow-linewidth system, with a size of 25 cm × 20cm × 13 cm and a weight of < 10 lb. The ruler is 1 foot long.*

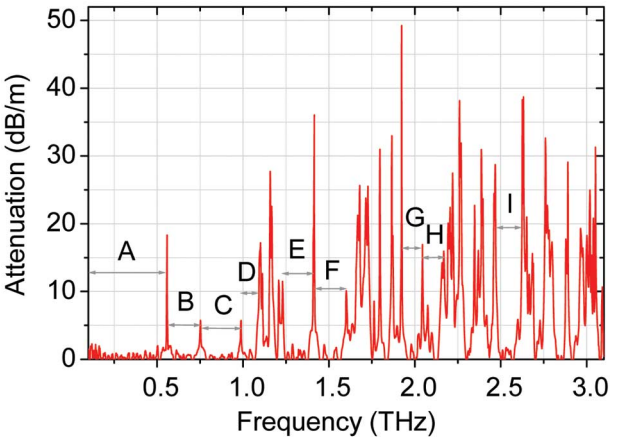


**Fig. 2.** *Atmospheric attenuation of THz waves in the range of 0.1–3 THz and nine major THz transmission bands. A: 0.1–0.55 THz; B: 0.56–0.75 THz; C: 0.76–0.98 THz; D: 0.99–1.09 THz; E: 1.21–1.41 THz; F: 1.42–1.59 THz; G: 1.92–2.04 THz; H: 2.05–2.15 THz; I: 2.47–2.62 THz. The temperature of the measurements was 23 °C, and the relative humidity was 26%.*

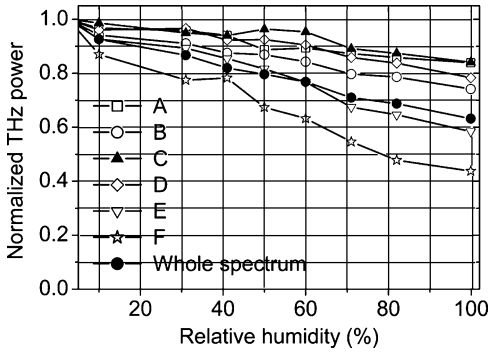


**Fig. 3.** *Transmitted THz power in the six transmission bands versus relative humidity.*

water vapor absorption in the THz band. We conducted a full experimental investigation on the propagation of THz waves in air and found a number of THz transmission windows, as shown in Fig. 2. The ranges between two water vapor absorption peaks are THz transmission windows. Nine major transmission windows throughout the 0.1–3 THz range are indicated.

We also conducted measurements of the THz transmission in different humidity. Fig. 3 contains plots of the transmitted THz power (integration over the corresponding range) in the six transmission bands versus relative humidity. The THz transmission decreases with the relative humidity. The transmission below ~1 THz is higher than that beyond 1 THz. Fig. 4. illustrates the THz spectra after different propagation distances in the atmosphere. The transmission bands become narrower as the propagation distance increases; however, reasonable bandwidths remain, even when the propagation distance reaches 108 m. The attenuation below ~0.65 THz is from beam divergence due to diffraction, not from the atmosphere. In addition, our measurements using Fourier transform far-infrared spectrometer indicates that THz waves in the 10.7–21 THz range also have low atmospheric attenuation. Any chemical or biological agents with THz fingerprints in these transmission bands will be detectable with THz waves at long standoff distances in the atmosphere.

## IV. SENSING WITH THz SPECTROSCOPY

Spectroscopic technologies are essential for chemical and biological sensing. THz technologies developed in the past decade such as THz-TDS enable us to explore spectroscopic sensing in the THz range.

### A. THz Spectra Database of ERCs

We measured the THz spectra of 15 ERCs with a THz-TDS system and a Fourier transform infrared (FTIR) spectrometer (Bruker IFS 66 V/S) in the 0.1–21 THz

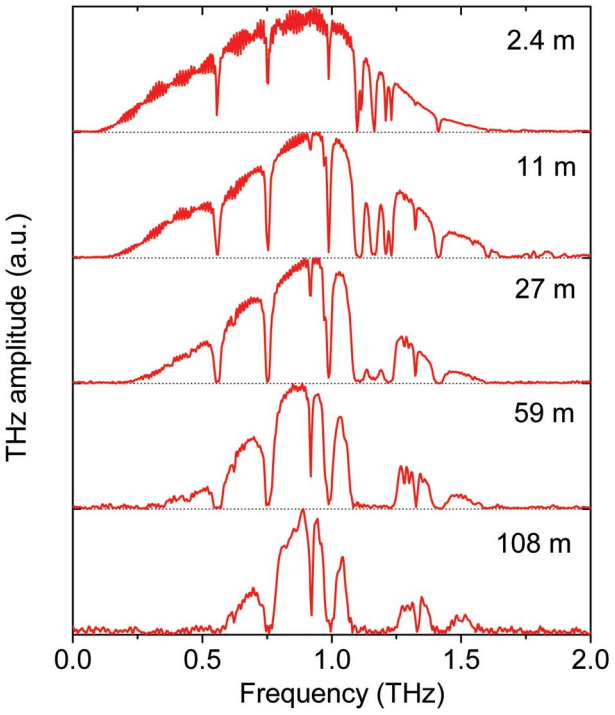


**Fig. 4.** *THz spectra at different propagation distances. The temperature of measurements was 22 °C, and the relative humidity was about 10%.*

(4–700 $cm^{-1}$) range, in a vacuum or a nitrogen purged environment. These samples include TNT, RDX, HMX, PETN, tetryl (2,4,6-trinitrophenyl- n-methylnitramine), 2-amino-4,6-DNT (2- amino-4,6-dinitro- toluene), 4-amino-2,6-DNT, 4-nitrotoluene, 1,3,5-TNB (1,3,5-trinitro-benzene), 1,3-DNB (1,3-dinitro-benzene), 1,4-DNB, 2,4-DNT, 2,6-DNT, 3,5-dinitro aniline, and 2-nitro diphenyl anine. Table 1 shows a summary of the absorption peak positions. Some of our data agree with the literature results [3], [5], [53] and some others are new observations. In Fig. 5, we compared the experimental results with the calculated results obtained using Gaussian 03 based on density functional theory. Most of these absorption features in the 3–21 THz range are from the normal vibrational modes of ERCs molecules according to the calculations. The experimental results include transmission spectra and diffuse reflectance spectra in the 1.5–21 THz range obtained with a FTIR spectrometer. Good agreements were achieved among calculated results, transmission, and diffuse reflection spectra. In the range of 0.1–3.0 THz, compared with FTIR spectrometer, THz-TDS has advantages such as a higher SNR without using a liquid-helium cooled bolometer detector. Therefore we measured the absorption spectra of common ERCs in the 0.1–3 THz range using THz-TDS in a nitrogen environment, as shown in Fig. 6. Most of these low frequency absorption fingerprints are from lattice vibrations or phonon modes of crystalline ERCs. There are also several ERCs that do not contain THz absorption features in the range of 0.1–3 THz, such as tetryl, 1,3,5-TNB, 1,4-DNB

Table 1 THz Absorption Peaks (THz) of ERCs

| Explosive & Related Compound | Measured Absorption Peak Position (THz) |
|---|---|
| TNT | 1.66, 2.20, 3.69, 4.71, 5.52, 8.28, 9.12, 9.78, 10.65, 11.01,13.86, 15.15, 16.95, 17.37, 19.17, 19.89 |
| RDX | 0.82, 1.05, 1.50, 1.96, 2.20, 3.08, 6.73, 10.35, 11.34, 12.33, 13.86, 14.52, 17.74, 18.12, 20.13 |
| HMX | 1.78, 2.51, 2.82, 5.31, 6.06, 11.28, 12.00, 12.54, 12.96, 13.74, 14.55, 18.15, 18.60, 19.38 |
| PETN | 2.0, 2.84 |
| Tetryl | 5.97, 10.11, 11.28, 14.67, 16.14, 18.36 |
| 2-amino-4, 6-DNT | 0.96, 1.43, 1.87, 3.96, 5.07, 6.27, 8.49, 9.87, 10.77, 12.15, 13.44, 16.68 |
| 4-amino-2, 6-DNT | 0.52, 1.24, 2.64, 3.96, 5.04, 5.82, 7.53, 9.30, 10.20, 11.13, 13.86, 14.97, 17.70 |
| 4-Nitrotoluene | 1.20, 1.37, 1.86, 6.75, 8.85, 10.83, 14.04, 15.66, 18.51 |
| 1,3,5-TNB | 4.17, 4.62, 10.05, 11.19, 13.80, 15.75, 19.05 |
| 1,3-DNB | 0.94, 1.19, 2.37, 10.56, 12.18, 15.33, 17.13 |
| 1,4-DNB | 3.24, 3.96, 5.55, 10.38, 12.45, 13.29, 15.21, 15.54 |
| 2,4-DNT | 0.45, 0.66, 1.08, 2.52, 4.98, 8.88, 10.56, 11.58, 12.81, 14.34, 15.69, 19.05, 20.04 |
| 2,6-DNT | 1.10, 1.35, 1.56, 2.50, 5.61, 6.75, 9.78, 11.43, 13.32, 13.89, 15.39, 17.25 |
| 3,5-dinitro aniline | 0.96, 1.20, 3.18, 4.62, 5.04, 5.91, 7.44, 10.62, 10.98, 14.46, 16.41, 18.18 |
| 2-nitro diphenyl anine | 2.19, 2.58, 2.88, 3.45, 5.13, 6.18, 7.56, 10.08, 12.33, 13.05, 15.00, 15.60, 16.29, 17.34, 18.51, 19.32 |

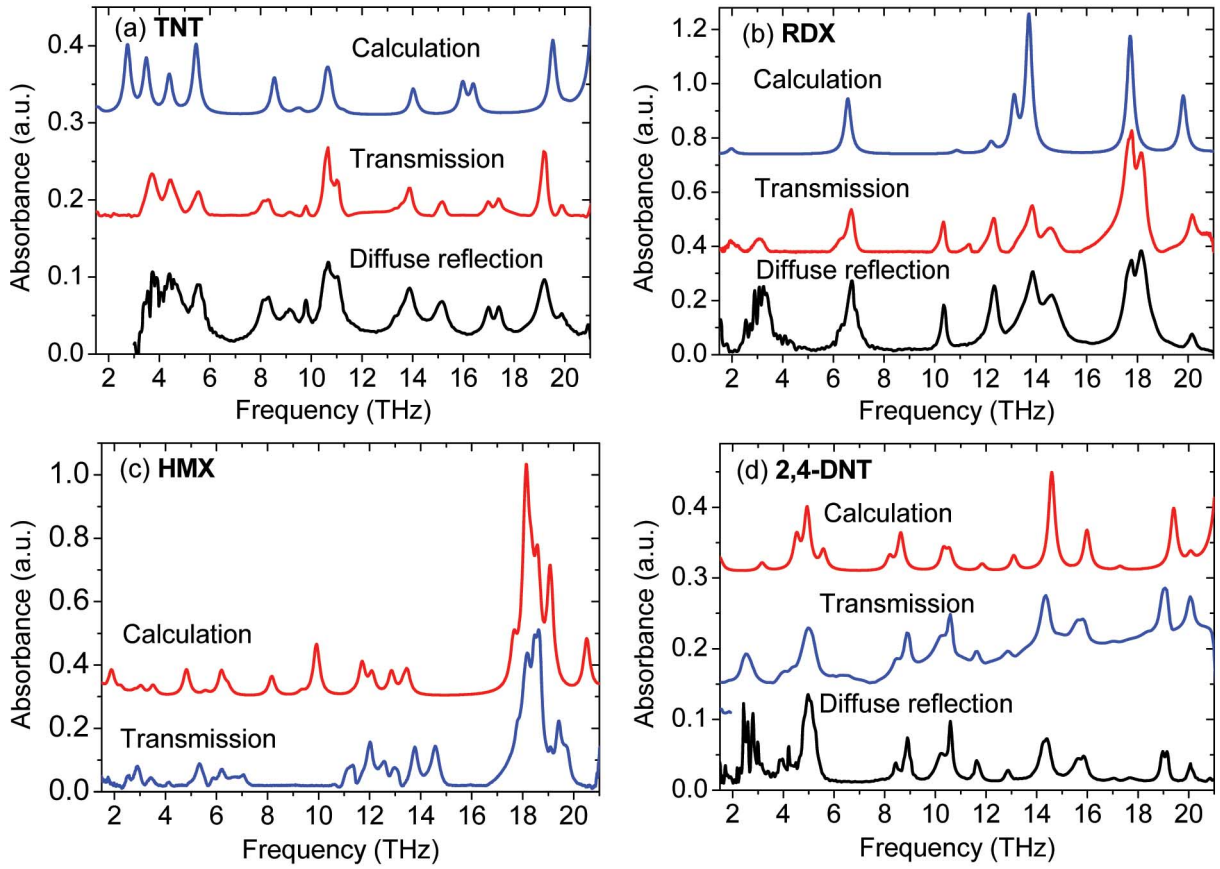


**Fig. 5.** ***Comparison of calculated results, transmission spectra, and diffuse reflectance spectra of: (a) TNT, (b) RDX, (c) HMX, and (d) 2, 4-DNT measured with FTIR. The spectra have been vertically shifted for clarity [4].***

according to our measurements. An additional example is ammonium nitrate which was reported previously [54]. However, they have fingerprints in the range of 3–21 THz. The detection of these ERCs requires special considerations since THz waves in the higher frequencies have lower penetration depths for many commonly used materials and their atmospheric attenuation is also different from those in the 0.1–3.0 THz range.

If a real-world scenario is considered, both atmospheric attenuation and a scattering effect will have significant effects on spectroscopic results. Therefore, THz sensing in the transmission windows is necessary for the real-world applications. ERCs have many distinguishable THz fingerprints in the range of 10.7–21 THz where THz waves also have low atmospheric attenuation. However, THz waves in this range do not have high penetration depths for many commonly used materials compared with those of lower frequency ranges. Therefore standoff detection in the range of 10.7–21 THz will be limited to exposed explosives. ERCs have abundant THz fingerprints in the 0.1–3 THz range where many commonly used materials become much more transparent. Therefore standoff detection of hidden explosives behind barriers in 0.1–3 THz range is more promising. To better employ these THz fingerprints of ERCs and mitigate atmospheric attenuation, further investigations need to be conducted. Sensing with narrow-linewidth CW THz waves is another promising direction. An array of CW sources and detectors covering a range wherein ERCs have THz fingerprints and the atmosphere has low attenuation will be applicable for standoff sensing.

### B. Detection of RDX by Diffusely Reflected THz Waves

Many groups have applied THz spectroscopy for explosives detection in transmission mode [3]–[6]. However, for practical applications, reflection measurements are preferred since most bulky targets are impossible to measure in a transmission mode. In addition, reflection spectroscopy, especially diffuse reflection spectroscopy is more applicable for standoff detection. Detection of RDX by THz spectroscopic imaging based on specular reflection has been demonstrated by Shen *et al.* recently [7]. However, in a real-world scenario, the targets usually have

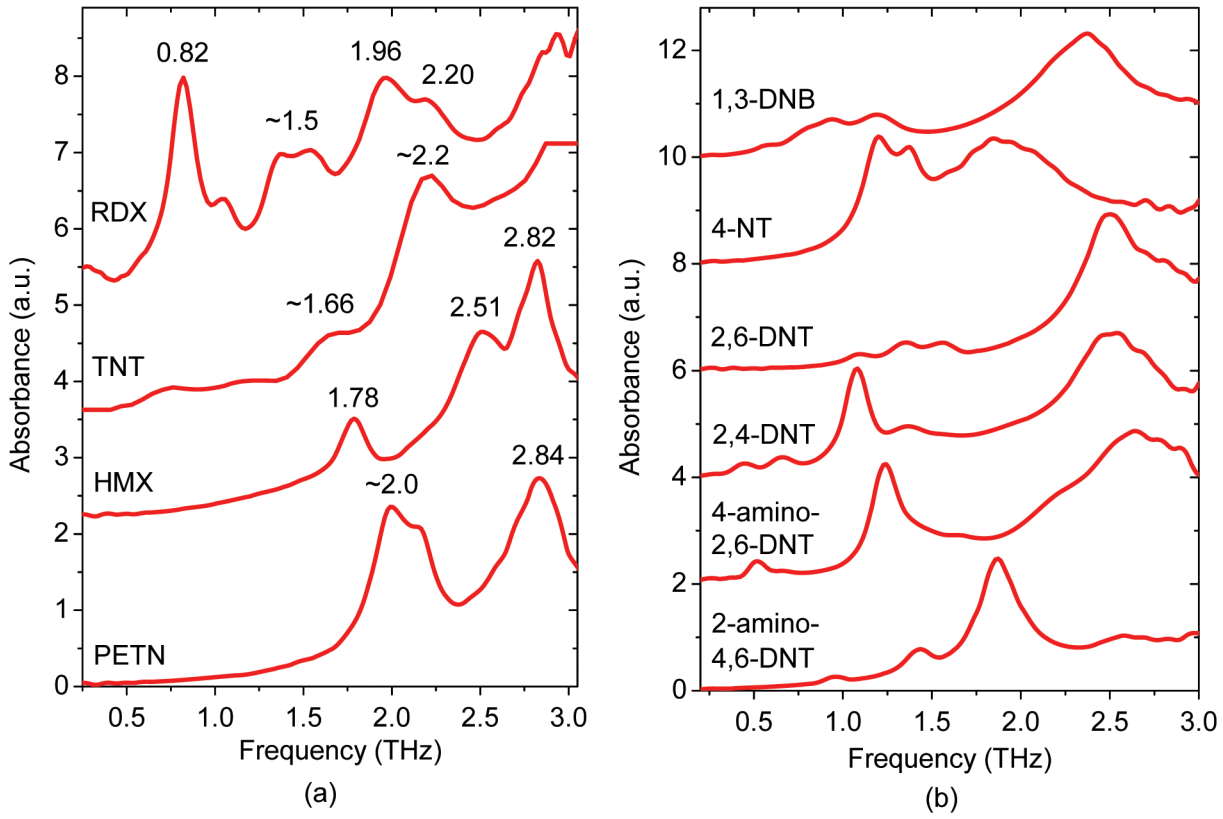


**Fig. 6.** *(a) THz absorption spectra of RDX, TNT, HMX. and PETN obtained with THz-TDS. (b) THz absorption spectra of explosive related compounds obtained using THz-TDS. The spectra have been vertically shifted for clarity.*

rough surfaces and the surfaces are not aligned normal to the THz beam, therefore the direction of the specular reflection is hard to determine. It is more feasible and realistic to detect and identify explosives by diffusely reflected THz waves. We applied THz-TDS to study diffuse reflection spectroscopy of explosives using RDX as a model compound [8]. Our investigation implies that THz diffuse reflection spectroscopy has a potential for the standoff detection and identification of explosives concealed in packages or under clothing.

With THz-TDS the complex refractive index of a sample can be obtained without using the Kramers–Kronig (K-K) transform. In a reflection mode, since the phase of the THz pulse depends on the position of the reflected surface, an accurate phase measurement requires a reference reflector exactly in the same position as the sample. The reference reflector should have a very similar surface morphology as the sample as well. In practical applications, this match is hard to achieve. Hence for the samples that are not optically smooth for THz waves, the retrieval of phase information from the time-domain signal is hard in reflection measurements and this has also been proved using our data. Considering this difficulty, we discarded phase information obtained in diffuse reflection measurements.

The reflection spectrum of a RDX pellet was acquired from a diffuse reflection measurement using a THz-TDS system in combination with a diffuse reflectance accessory. A Teflon (almost transparent for THz waves) pellet and was used as a reference. The measurements were conducted in a chamber purged with nitrogen to avoid the influence of water vapor absorption in ambient air. In the experiments, one quarter of all the diffusely reflected THz radiation (in $\sim$1/8 of a spherical space) from the RDX sample surface was collected by an off-axis ellipsoidal mirror. The absorption spectrum (0.2–1.8 THz) obtained by applying the Kramers-Kronig (K-K) transform to the reflection spectrum agrees with that from a transmission measurement, as shown in Fig. 7(a). Two common materials without THz absorption features, polyethylene and flour, were also tested using the same system to compare with RDX, as plotted in Fig. 7(b). There were some small spectral variations in the absorption spectra of polyethylene and flour, as shown in Fig. 7(b). This finding differs from the result obtained from the transmission measurements of polyethylene and flour, which have no THz absorption features. We attribute the discrepancy to differences in the surface roughness of the samples (polyethylene or flour) and reference (Teflon).

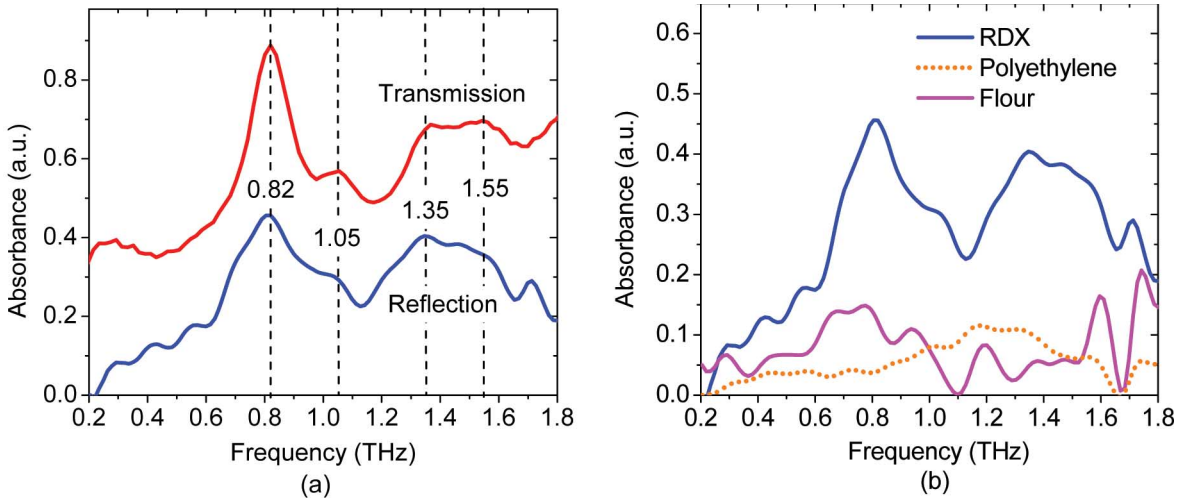


**Fig. 7.** *(a) The comparison between the absorption spectrum from the transmission measurement (upper curve) and that from the diffuse reflection measurement (bottom curve).The transmission spectrum has been vertically shifted for clarity. (b) Absorption spectra of RDX, polyethylene, and flour from the K-K transform of the reflection spectra. All the measurements were conducted in a nitrogen-purged environment to avoid the effects of water vapor absorptions in ambient air [8].*

In order to demonstrate the abilities of THz spectroscopy for the detection of hidden explosives, we have also investigated the THz diffuse reflection spectroscopy of RDX under covering materials. The RDX samples were covered with four different barrier materials, paper (thickness: ~0.05 mm, white), polyethylene (~0.1 mm, black), leather (~0.3 mm, yellow), and polyester cloth (~0.4 mm, green), which are all opaque for visible light. The measurements were conducted in ambient atmosphere (with a relative humidity of ~20%) instead of nitrogen. The absorption spectra obtained from the K-K transform are shown in Fig. 8. In ambient atmosphere, water vapor absorption affected the measurements, especially in the range above 1.0 THz. In addition, the barrier materials also led to the distorted spectral band shapes and shifts of absorption peaks. Due to water vapor

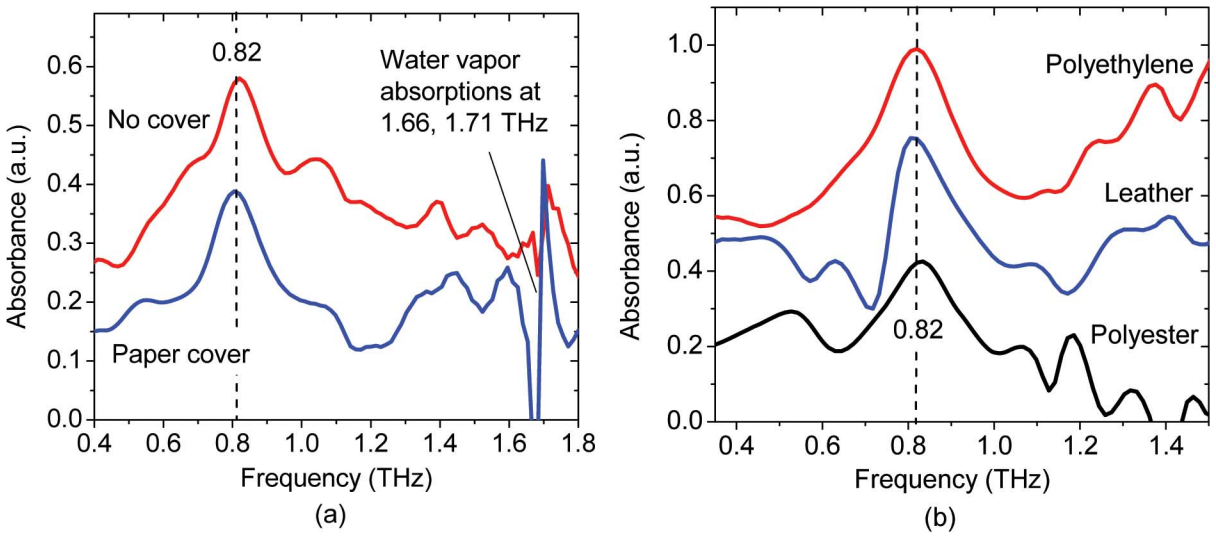


**Fig. 8.** *(a) A comparison between the absorption spectra of RDX obtained from the diffuse reflection measurements when RDX was bare and was covered with paper. (b) Absorption spectra of RDX obtained from the diffuse reflection measurements under different covers. Upper curve: polyethylene sheet cover; middle curve: leather cover; bottom curve, polyester cloth cover. The spectra have been vertically shifted for clarity [8].*

absorption and covering material effects, many of the weak absorption features of RDX cannot be identified, and there are even artifact features. However, the absorption peak at 0.82 THz is always observed behind all barriers in the atmosphere. This investigation demonstrates that the THz technique is a feasible tool for detecting hidden RDX-related explosives, such as C-4 under clothing or inside packages in diffuse reflection geometry.

### C. Standoff Sensing RDX by Specularly Reflected THz Waves

Standoff detection involves passive and active methods for sensing chemical and biological materials when the sensor is physically separated from the target. Although many techniques and methodologies are available for explosive screening when close proximity is possible, standoff distance (several meters) sensing of explosives is as a bottleneck [55], [56]. Many of the existing standoff methods either are invasive to the suspect personnel (e.g., X-ray and Raman spectroscopy) or lack spectroscopic features for explosive materials (e.g., thermal infrared detection). THz-TDS is a potential modality, but suffers from blind regions in the spectrum due to water vapor absorption lines [57], [58]. To demonstrate the feasibility of a pulsed THz standoff sensing system, RDX was chosen in our investigations as it has a prominent absorption peak at around 0.82 THz, between two water absorption lines centered at 0.75 and 0.99 THz. To make a comparison, polyethylene, a material which does not have any THz absorption features, was also tested with the standoff sensing system. A metal mirror was used as a reference.

The experimental setups were THz-TDS with different THz propagation distances. The THz beam propagated in ambient air for a certain distance (2.5–30 m) and was focused onto the sample with a small incident angle (less than 10°) by a parabolic mirror. The specularly reflected THz waves from the sample were then collected by another parabolic mirror and collimated to travel back to the THz detector for another certain distance (2.5–30 m).

The propagation distance of the probe beam in THz-TDS was reduced by taking advantage of the high repetition rate of the femtosecond laser. Since the repetition rate of the laser is 80 MHz, the spatial delay between two adjacent pulses is 3.75 m. So for a certain propagation distance of $>3.75$ m, the subsequent pulses will be used to detect the THz pulse. As an example, for 30 m, the 59th pulse $(30 \times 2/3.75 - 1)$ after the pumping pulse was used as probe pulse. A short propagation distance of probe beam decreased its noise level.

Although the arrangement of the two parabolic mirrors is not practical in real-world applications, it ensured collection efficiency given the limited amount of explosive sample material (a 1.5 mm-thick pellet with a diameter of about 13 mm). This study provides a situation in which one is able to demonstrate the concept of standoff sensing explosives with THz-TDS. Generally, highly explosive materials, such as RDX, PETN, and HMX, are stored in relatively large amounts. In that case, the reflected THz signal can be collected using more sophisticated large aperture collectors, such as a Cassegrain telescope [59].

In our study, the reflected THz pulses from RDX and polyethylene pellets were measured and their absorption spectra were calculated using the relative reflectance and phase change profiles that were readily accessible using THz-TDS. The results are illustrated in Fig. 9. The absorption peak of RDX centered at 0.82 THz was identified at a standoff distance up to 30 m. It is noteworthy that artificial spikes appeared around water absorption lines (at 0.56, 0.75, and 0.99 THz) which make the curves like the index of refraction. These spikes resulted from the variation of relative humidity and the water vapor absorption saturation, which lead to very low SNR at these frequencies thus the abnormal data points in absorption.

We also estimated the standoff distance limit based on the dynamic range of the phase change. For many organic compounds, the extinction coefficient $k$ is usually much

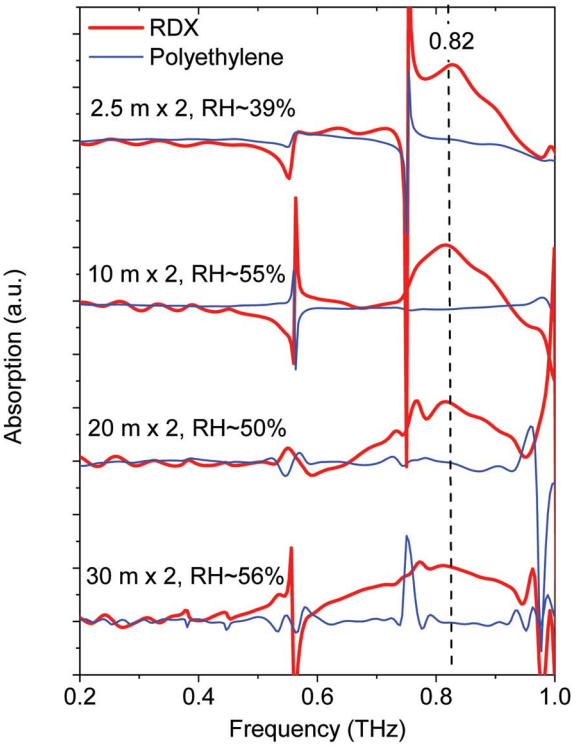


**Fig. 9.** *The absorption spectra of RDX (black line) and polyethylene (gray line) for different sensing distances in different relative humidity (RH). The dash line indicates the absorption peak round 0.82 THz. The spikes around 0.38, 0.44, 0.56, 0.75, and 0.99 THz are due to the fluctuations of water vapor in the atmosphere [9].*

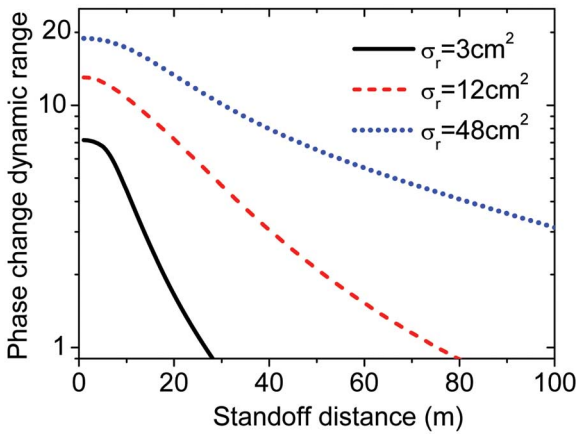


**Fig. 10.** *Phase change dynamic range calculated against standoff distance, with different sizes of RDX reflection areas.*

smaller than the refractive index $n$ [60], therefore their phase change and extinction coefficient (or absorption coefficient) show similar behavior around resonant frequencies. For instance, in the phase change profile of RDX, there is also a strong peak around 0.82 THz, with a peak value of approximately 0.5 radians. Hence the background phase noise at 0.82 THz determines the visibility of the standoff detection of RDX. Our calculation showed that phase noise was mainly attributed to amplitude degradation of the signal, if the scan rate was so fast that humidity, temperature, and ranging drift were not considered. By assuming a Gaussian propagation model with an emission divergence angle of 0.03 radians, and a "phase change dynamic range" (peak phase change over phase noise) of 20 at 0.82 THz at a close distance (< 1 m), we predicted the standoff distance limit for various sizes of RDX reflection area by plotting the phase change dynamic range against the standoff distance. The result is illustrated in Fig. 10. It reveals that, with 3 $cm^2$ reflection area, the dynamic range of phase change reaches 1, indicating 30 m is the standoff detection limit under the above circumstances.

## V. IMAGING WITH THz WAVES

### A. Imaging With Pulsed THz Waves

The main advantages of imaging with pulsed THz waves by THz-TDS include the broadband nature, noninvasiveness, and coherent detection.

The earliest pulsed THz imaging experiment was done by raster scanning the sample with a focused THz beam [61]. In this method, the change in refractive index is shown in the timing and phase of the pulse, whereas the density variation modulates the pulse peak amplitude. By analyzing the THz pulse in the frequency domain, one is able to identify materials with characteristic features in the THz spectrum. This raster scan configuration has been widely adopted in applications such as biomedical diagnosis [62], the imaging and sensing of drugs [63], explosives and landmines [64], and nondestructive defect identifications [65], [66].

Another remarkable imaging method is pulsed THz tomography. THz tomography refers to the imaging technology in which either reflected or transmitted THz wave illumination reveals the cross section image of the object. Raster scanning pulsed THz imaging in reflection geometry can be considered tomography, as it renders 3-D profiles of a layered structure by recording pulses reflected from each interface [67]. For example, in our lab we have applied this technique to inspect space shuttle insulation foam, as the defected interface area modulates the pulses in both time and frequency domain. Pulsed THz computed tomography is the THz region adaptation of X-ray tomography [68]. It is able to reconstruct the reflective index and density image by taking inverse radon transforms of both the phase and amplitude of the transmitted THz pulse. Pulsed THz binary lens tomography benefits from the frequency-dependent focal length of Fresnel binary lenses, so that the images at different depths are projected on a single imaging plane by their correspondent frequencies that satisfy the lens equation [69].

THz 2-D EO imaging is a big leap forward from the traditional raster scan imaging [70]. In this technique, the entire THz field modulates an expanded probe beam onto a large EO sensor crystal. The modulated beam profile is captured by a CCD camera. It greatly improves data acquisition speed and makes real-time THz imaging possible. Spectroscopic 2-D THz EO imaging has been reported [71], however, field tests are facing hurdles due to insufficient SNR.

Other pulsed THz imaging modalities include THz impulse synthetic aperture radar imaging [72], THz interferometric imaging [73], and THz reflection multistatic imaging using Kirchhoff migration [74], etc. Many of them benefit from technologies that are well-developed, such as radar astronomy, microwave holography, and ultrasound technology.

### B. Imaging With CW THz Radiation

An area of increasing interest in the THz field in recent years has been the generation and use of CW THz radiation. Imaging with CW THz radiation actually predates pulsed THz imaging [75], but activity in the field has only been revived recently. CW THz imaging is advantageous compared with pulsed THz imaging for specific defense applications due to its higher single-frequency dynamic range and the nature of possessing a narrow spectral width. Whereas the energy of a pulse is spread over a broad spectrum, causing a significant amount to be lost due to water vapor absorption, a CW system

tuned to spectral windows between atmospheric absorption lines is easier to operate at longer standoff distances. In addition, because no time-delay scan is required in a CW system, the speed of a CW THz imaging system can be increased relative to that of a pulsed system, in which time-delay scanning is necessary.

Various methods of generating CW THz waves have been utilized for imaging purposes, including frequency-multiplied microwave sources [76], backward wave oscillators [77], quantum cascade lasers [78], $CO_2$-pumped THz gas lasers, photomixing [79], and THz-wave parametric oscillators [10]. Spectral information can also be retrieved with a CW THz imaging system which is continuously tunable over a large bandwidth, such as photomixing, and THz-wave parametric oscillators. However, for many applications, information regarding the transmitted intensity is all that is required, and using powerful single frequency CW radiation is advantageous over broadband waves.

Imaging with a CW system requires a method for associating the radiation received with its location in space. There are two methods that are commonly used: a raster scan of a focused beam, or the formation of an image on a detector array. In the former, a single detector, such as a Schottky diode, Golay cell, or pyroelectric detector is used to detect the full power of the beam. This has the advantage of a high dynamic range, but the disadvantage that the image must be formed point by point using a scanning system, which is time-consuming and not applicable to moving targets. The development of a sensitive THz detector array is still an active area. Pyroelectric arrays are commercially available, but their sensitivity in the THz range is poor and they are too small to provide high-resolution images of large targets. Detector arrays also have the disadvantage of being severely affected by distortions and aberrations in the focusing system, whereas for a raster scanning system, the beam can easily be focused to a diffraction-limited spot.

We have tested CW THz imaging's potential for two applications areas: nondestructive testing and security screening. The results shown utilize a raster-scanning method for the formation of the image, frequency-multiplied Gunn diode oscillators as the sources, and a Golay cell as the detector. During the experiments, the standing wave effect was avoided by constructing a destructive interference in the other path of the 50/50 beam splitter. In Fig. 11, a 0.2 THz scan of a briefcase containing a variety of items is displayed. Most of the nonconducting material of which the briefcase is composed is transparent enough to THz radiation for an image to be formed. The metallic items present block the radiation completely and are recognizable only as silhouettes. Such a scan takes approximately 8 min to complete, which is obviously too long for real-world applications, but the potential for the technology, given improvements in imaging speed, is undoubted.

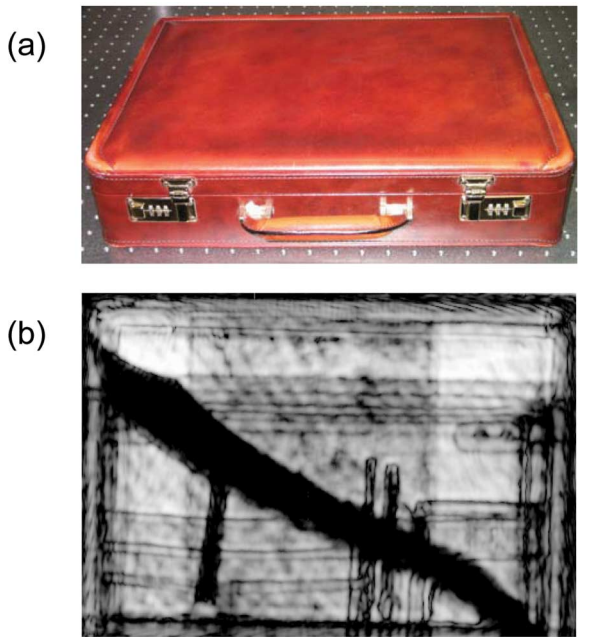


**Fig. 11.** *(a) Optical image of a leather briefcase containing pens, a magazine, and a large knife. (b) 0.2 THz image of the briefcase.*

In Fig. 12, an image of a shoe scanned with CW THz radiation is shown. The structure of the shoe is visible, including that of the rubber sole. This may be of interest in the field of airport security, as the nonionizing nature of

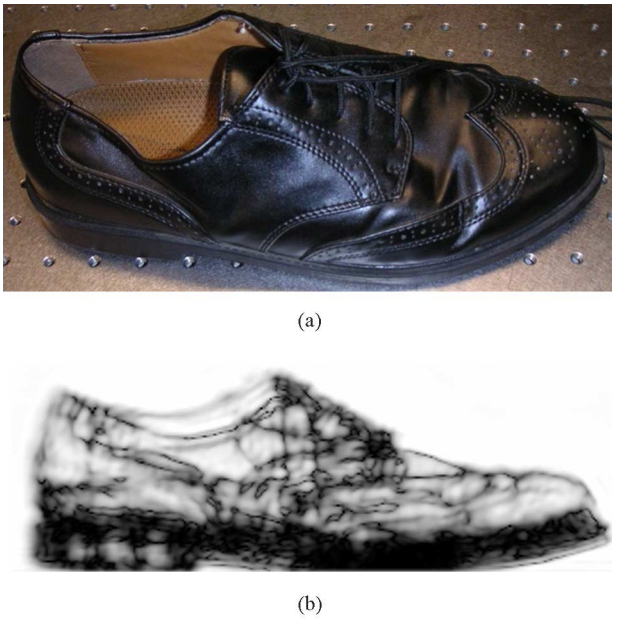


**Fig. 12.** *(a) Optical image of a shoe. (b) 0.2 THz scan of the shoe, revealing the structure.*

THz radiation could make it possible to perform scans of such articles while their owners are still wearing them.

These results indicate that CW THz imaging is capable of accessing useful information for security applications. With expected improvements to imaging speed, CW THz imaging may become a complementary technology to X-ray scanning for security applications.

## VI. CONCLUSION

The most recent developments in THz technology and new explorations of THz spectroscopy and imaging have advanced THz applications in the defense and security fields. Critical to the successful implementation of these THz applications include well-developed THz technologies, an establishment of more comprehensive THz spectral database for both ERCs and commonly used materials, standoff detection and identification of ERCs in reflection modes using narrowband CW THz systems, and the optimized data screening algorithm. There are still challenges and obstacles to implement THz technologies for defense and security in real-world applications. Powerful THz sources and sensitive THz detection methods need further development. Theoretical calculations of the THz phonon modes remain as an unsolved problem. Atmospheric attenuation and scattering effects greatly influence THz sensing results. However, THz science and technology has already shown great potential. Together with worldwide investigations, our THz sensing and imaging results indicate THz technologies will play more and more important roles in defense and security applications. ■

## Acknowledgment

The authors would like to thank Jingzhou Xu, Albert Redo, Brian Schulkin, Glenn Bastiaans, Robert Osiander, James Spicer, and Badri Roysam for their technical support and critical discussions.

## REFERENCES

[1] M. R. Scarfi, M. Romanò, R. Di Pietro, O. Zeni, A. Doria, G. P. Gallerano, E. Giovenale, G. Messina, A. Lai, G. Campurra, D. Coniglio, and M. D'Arienzo, "THz exposure of whole blood for the study of biological effects on human lymphocytes," *J. Biol. Phys.*, vol. 29, pp. 171–177, 2003.

[2] R. H. Clothier and N. Bourne, "Effects of THz exposure on human primary keratinocyte differentiation and viability," *J. Biol. Phys.*, vol. 29, pp. 171–185, 2003.

[3] M. C. Kemp, P. F. Taday, B. E. Cole, J. A. Cluff, A. J. Fitzgerald, and W. R. Tribe, "Security applications of terahertz technology," *Proc. SPIE*, vol. 5070, pp. 44–52, 2003.

[4] Y. Chen, H. Liu, Y. Deng, D. Veksler, M. Shur, X.-C. Zhang, D. Schauki, M. J. Fitch, and R. Osiander, "Spectroscopic characterization of explosives in the far infrared region," *Proc. SPIE*, vol. 5411, pp. 1–8, 2004.

[5] K. Yamamoto, M. Yamaguchi, F. Miyamaru, M. Tani, M. Hangyo, T. Ikeda, A. Matsushita, K. Koide, M. Tatsuno, and Y. Minami, "Noninvasive inspection of C-4 explosive in mails by terahertz time-domain spectroscopy," *Jpn. J. Appl. Phys.*, vol. 43, pp. L414–L417, 2004.

[6] F. Huang, B. Schulkin, H. Altan, J. F. Federici, D. Gary, R. Barat, D. Zimdars, M. Chen, and D. B. Tanner, "Terahertz study of 1,3,5-trinitro-s-triazine by time-domain and Fourier transform infrared spectroscopy," *Appl. Phys. Lett.*, vol. 85, pp. 5535–5537, 2004.

[7] Y. C. Shen, T. Lo, P. F. Taday, B. E. Cole, W. R. Tribe, and M. C. Kemp, "Detection and identification of explosives using terahertz pulsed spectroscopic imaging," *Appl. Phys. Lett.*, vol. 86, p. 241 116, 2005.

[8] H. B. Liu, Y. Chen, G. J. Bastiaans, and X.-C. Zhang, "Detection and identification of explosive RDX by THz reflection spectroscopy," *Opt. Express*, vol. 14, pp. 415–423, 2006.

[9] H. Zhong, A. Redo, and X.-C. Zhang, *THz standoff detection of explosive RDX*, unpublished work.

[10] K. Kawase, "Terahertz imaging for drug detection and large-scale integrated circuit inspection," *Opt. Photon. News*, pp. 34–39, Oct. 2004.

[11] E. L. Saldin, E. A. Schneidmiller, and M. V. Yurkov, *The Physics of Free Electron Lasers, Advanced Texts in Physics*. New York: Springer-Verlag, 2000, Berlin.

[12] M. van Exter and D. Grischkowsky, "Characterization of an optoelectronic terahertz beam system," *IEEE Trans. Microw. Theory Tech.*, vol. 38, no. 11, pp. 1684–1691, Nov. 1990.

[13] N. Sarukura, H. Ohtake, S. Izumida, and Z. L. Liu, "High average-power THz radiation from femtosecond laser-irradiated InAs in a magnetic field and its elliptical polarization characteristics," *J. Appl. Phys.*, vol. 84, pp. 654–657, 1998.

[14] M. Nakajima, M. Takahashi, and M. Hangyo, "Strong enhancement of THz radiation intensity from semi-insulating GaAs surfaces at high temperatures," *Appl. Phys. Lett.*, vol. 81, pp. 1462–1464, 2002.

[15] G. Zhao, R. N. Schouten, N. van der Valk, W. T. Wenckebach, and P. C. M. Planken, "Design and performance of a THz emission and detection setup based on a semi-insulating GaAs emitter," *Rev. Sci. Instrum.*, vol. 73, pp. 1715–1719, 2002.

[16] H.-M. Heiliger, M. Vossebürger, H. G. Roskos, H. Kurz, R. Hey, and H. Kurz, "Application of liftoff low-temperature-grown GaAs on transparent substrates for THz signal generation," *Appl. Phys. Lett.*, vol. 69, pp. 2903–2905, 1996.

[17] M. Tani, S. Matsuura, K. Sakai, and S. Nakashima, "Emission characteristics of photoconductive antennas based on low-temperature-grown GaAs and semi-insulating GaAs," *Appl. Opt.*, vol. 36, pp. 7853–7859, 1997.

[18] P. Gu, M. Tani, S. Kono, K. Sakai, and X.-C. Zhang, "Study of terahertz radiation from InAs and InSb," *J. Appl. Phys.*, vol. 91, pp. 5533–5537, 2002.

[19] H. Takahashi, A. Quema, M. Goto, S. Ono, and N. Sarukura, "Terahertz radiation mechanism from femtosecond-laser-irradiated InAs (100) surface," *Jpn. J. Appl. Phys.*, vol. 42, pp. L1259–L1261, 2003.

[20] Q. Wu, M. Litz, and X.-C. Zhang, "Broadband detection capability of ZnTe electro-optic field detectors," *Appl. Phys. Lett.*, vol. 68, pp. 2924–2926, 1996.

[21] A. Rice, Y. Jin, X. F. Ma, X.-C. Zhang, D. Bliss, J. Larkin, and M. Alexander, "Terahertz optical rectification from (110) zinc-blende crystals," *Appl. Phys. Lett.*, vol. 64, pp. 1324–1326, 1994.

[22] K. Reimann, R. P. Smith, A. M. Weiner, T. Elsaesser, and M. Woerner, "Direct field-resolved detection of terahertz transients with amplitudes of megavolts per centimeter," *Opt. Lett.*, vol. 28, pp. 471–473, 2003.

[23] R. Huber, A. Brodschelm, F. Tauser, and A. Leitenstorfer, "Generation and field-resolved detection of femtosecond electromagnetic pulses tunable up to 41 THz," *Appl. Phys. Lett.*, vol. 76, pp. 3191–3193, 2000.

[24] K. H. Yang, P. L. Richards, and Y. R. Shen, "Generation of far-infrared radiation by picosecond light pulses in $LiNbO_3$," *Appl. Phys. Lett.*, vol. 19, pp. 320–323, 1971.

[25] T. J. Carrig, G. Rodriguez, T. S. Clement, A. J. Taylor, and K. R. Stewart, "Scaling of terahertz radiation via optical rectification in electro-optic crystals," *Appl. Phys. Lett.*, vol. 66, pp. 121–123, 1995.

[26] A. M. Sinyukov and L. M. Hayden, "Generation and detection of terahertz radiation with multilayered electro-optic polymer films," *Opt. Lett.*, vol. 27, pp. 55–57, 2002.

[27] A. M. Sinyukov, M. R. Leahy, L. M. Hayden, M. Haller, J. Luo, A. K.-Y. Jen, and L. R. Dalton, "Resonance enhanced THz generation in electro-optic polymers near the absorption maximum," *Appl. Phys. Lett.*, vol. 85, pp. 5827–5829, 2004.

[28] P. Y. Han and X. C. Zhang, "Coherent, broadband mid-infrared terahertz beam sensors," *Appl. Phys. Lett.*, vol. 73, pp. 3049–3051, 1998.

[29] P. Y. Han, G. C. Cho, and X. C. Zhang, "Broad band mid-infrared THz pulse: Measurement technique and applications," *J. Nonlinear Opt. Phys. Mater.*, vol. 8, pp. 89–105, 1999.

[30] S. Kono, M. Tani, and K. Sakai, "Coherent detection of mid-infrared radiation up to 60 THz with an LT-GaAs photoconductive antenna," *IEE Proc. Optoelectron.*, vol. 149, p. 105, 2002.

[31] Y. C. Shen, P. C. Upadhya, H. E. Beere, E. H. Linfield, A. G. Davies, I. S. Gregory, C. Baker, W. R. Tribe, and M. J. Evans, "Generation and detection of ultrabroadband terahertz radiation using photoconductive emitters and receivers," *Appl. Phys. Lett.*, vol. 85, pp. 164–166, 2004.

[32] Q. Wu and X.-C. Zhang, "Free-space electro-optic sampling of terahertz beams," *Appl. Phys. Lett.*, vol. 67, pp. 3523–3525, 1995.

[33] A. Nahata, A. S. Weling, and T. F. Heinz, "A wideband coherent terahertz spectroscopy system using optical rectification and electro-optic sampling," *Appl. Phys. Lett.*, vol. 69, pp. 2321–2323, 1996.

[34] Q. Wu, M. Litz, and X.-C. Zhang, "Broadband detection capability of ZnTe electro-optic field detectors," *Appl. Phys. Lett.*, vol. 68, pp. 2924–2926, 1996.

[35] VDI Virginia Diodes, Inc. [Online]. Available: http://www.virginiadiodes.com

[36] Radiometer-Physics GmbH (RPG). Germany. [Online]. Available: http://www.radiometer-physics.de

[37] Microtech Instruments, Inc. [Online]. Available: http://www.mtinstruments.com

[38] Insight Product Co. [Online]. Available: http://www.insight-product.com

[39] Kawase Initiative Research Unit. [Online]. Available: http://www.riken.go.jp/lab-www/THz/

[40] E. R. Brown, F. W. Smith, and K. A. McIntosh, "Coherent millimetre-wave generation by heterodyne conversion in low-temperature-grown GaAs photoconductors," *Appl. Phys. Lett.*, vol. 73, pp. 1480–1482, 1993.

[41] E. R. Brown, K. A. McIntosh, K. B. Nichols, and C. L. Dennis, "Photomixing up to 3.8 THz in low-temperature GaAs," *Appl. Phys. Lett.*, vol. 66, pp. 285–287, 1995.

[42] J. E. Bjarnason, T. L. J. Chan, A. W. M. Lee, E. R. Brown, D. C. Driscoll, M. Hanson, A. C. Gossard, and R. E. Muller, "ErAs:GaAs photomixer with two-decade tenability and 12$\mu$W peak output," *Appl. Phys. Lett.*, vol. 85, pp. 3983–3985, 2004.

[43] C. Baker, I. S. Gregory, W. R. Tribe, E. H. Linfield, and M. Missous, "All-optoelectronic terahertz system using low-temperature-grown InGaAs photomixer," *Opt. Express*, vol. 13, pp. 9639–9644, 2005.

[44] Coherent Inc. [Online]. Available: www.coherent.com/Lasers/index.cfm?fuseaction=show.page&id=779&loc=834

[45] R. Köhler, A. Tredicucci, F. Beltram, H. E. Beere, E. H. Linfield, A. G. Davies, D. A. Ritchie, R. C. Iotti, and F. Rossi, "Terahertz semiconductor-heterostructure laser," *Nature*, vol. 417, pp. 156–159, 2002.

[46] L. Mahler, A. Tredicucci, R. Köhler, F. Beltram, H. E. Beere, E. H. Linfield, and D. A. Ritchie, "High-performance operation of single-mode terahertz quantum cascade lasers with metallic gratings," *Appl. Phys. Lett.*, vol. 87, p. 181 101, 2005.

[47] S. Kumar, B. S. Williams, S. Kohen, Q. Hu, and J. L. Reno, "Continuous-wave operation of terahertz quantum-cascade lasers above liquid-nitrogen temperature," *Appl. Phys. Lett.*, vol. 84, pp. 2494–2497, 2004.

[48] Virginia Diodes, Inc. [Online]. Available: http://www.virginiadiodes.com/mixers.htm

[49] Pacific Millimeter Products. [Online]. Available: http://www.pacificmillimeter.com/Mixers.html

[50] Microtech Instruments, Inc. [Online]. Available: http://www.mtinstruments.com/thzdetectors/index.htm

[51] Pacific Millimeter Products. [Online]. Available: http://www.pacificmillimeter.com/Detectors.html

[52] S. Hayashi, H. Minamide, T. Ikari, Y. Ogawa, K. Shindo, T. Shibuya, H. Sakai, H. Kan, T. Taira, H. Ito, C. Otani, and K. Kawase, "Palmtop terahertz-wave parametric generators," in *Conf. Dig. 2005 Joint 30th Int. Conf. Infrared and Millimeter Waves & 13th Int. Conf. Terahertz Electronics*, pp. 399–400, TC5-64.

[53] *Infrared Spectra*. Philadelphia, PA: Sadtler Res. Labs., 1980.

[54] D. J. Cook, B. K. Decker, G. Maislin, and M. G. Allen, "Through container THz sensing: Applications for explosive screening," *Proc. SPIE*, vol. 5354, pp. 55–62, 2004.

[55] J. E. Parrneter, "The challenge of standoff explosives detection," in *Proc. IEEE 38th Annu. 2004 Int. Carnahan Conf. Security Technology*, pp. 355–358.

[56] National Research Council, *Existing and Potential Standoff Explosives Detection Techniques*. Washington, DC: National Academy Press, 2004.

[57] M. K. Choi, A. Bettermann, and D. W. van der Weide, "Potential for detection of explosive and biological hazards with electronic terahertz system," *Phil. Trans. R. Soc. Lond. A*, vol. 362, pp. 337–349, 2004.

[58] A. J. Kemp, J. R. Birch, and M. N. Afsar, "The refractive index of water vapor: A comparison of measurement and theory," *Infrared Phys.*, vol. 18, pp. 827–833, 1978.

[59] J. C. Carter, S. M. Angel, M. Lawrence-Snyder, J. Scaffidi, R. E. Whipple, and J. G. Reynolds, "Standoff detection of high explosive materials at 50 meters in ambient light conditions using a small Raman instrument," *Appl. Spectrosc.*, vol. 59, pp. 769–775, 2005.

[60] M. Fox, *Optical Properties of Solids*. New York: Oxford, 2002.

[61] B. B. Hu and M. C. Nuss, "Imaging with terahertz waves," *Opt. Lett.*, vol. 20, pp. 1716–1718, 1995.

[62] R. Woodward, B. Cole, V. Wallace, R. Pye, D. Arnone, E. Linfield, and M. Pepper, "Terahertz pulse imaging in reflection geometry of human skin cancer and skin tissue," *Phys. Med. Biol.*, vol. 47, pp. 3853–3863, 2002.

[63] K. Kawase, Y. Ogawa, Y. Watanabe, and H. Inoue, "Non-destructive terahertz imaging of illicit drugs using spectral fingerprints," *Opt. Express*, vol. 11, pp. 2549–2554, 2003.

[64] H. Zhong, N. Karpowicz, J. Partridge, X. Xie, J. Z. Xu, and X. C. Zhang, "Terahertz wave imaging for landmine detection," *Proc. SPIE*, vol. 5411, pp. 33–44, 2004.

[65] D. Zimdars, J. Valdmanis, J. White, and G. Stuk, "Time domain terahertz detection of flaws within spaceshuttle sprayed on foam insulation *Tech. Dig. Conf. Lasers and Electro-Optics,*, 2004, paper CThN4.

[66] H. Zhong, J. Xu, X. Xie, T. Yuan, R. Reightler, E. Madaras, and X.-C. Zhang, "Nondestructive defect identification by terahertz time-of-flight tomography," *IEEE Sensors J.*, vol. 5, no. 2, pp. 203–208, Apr. 2005.

[67] D. M. Mittleman, S. Hunsche, L. Boivin, and M. C. Nuss, "T-ray tomography," *Opt. Lett.*, vol. 22, pp. 904–906, 1997.

[68] B. S. Ferguson, S. H. Wang, D. Gray, D. Abbot, and X.-C. Zhang, "T-ray computed tomography," *Opt. Lett.*, vol. 27, pp. 1312–1314, 2002.

[69] S. H. Wang and X.-C. Zhang, "Tomographic imaging with a terahertz binary lens," *Appl. Phys. Lett.*, vol. 82, pp. 1821–1823, 2003.

[70] Q. Wu, T. D. Hewitt, and X.-C. Zhang, "Two-dimensional electro-optic imaging of terahertz beams," *Appl. Phys. Lett.*, vol. 69, pp. 1026–1028, 1996.

[71] M. Usami, M. Yamashita, K. Fukushima, C. Otani, and K. Kawase, "Terahertz wideband spectroscopic imaging based on 2D electro-optic sampling technique," *Appl. Phys. Lett.*, vol. 86, p. 141 109, 2005.

[72] K. McClatchey, M. T. Reiten, and R. A. Cheville, "Time resolved synthetic aperture terahertz impulse imaging," *Appl. Phys. Lett.*, vol. 79, pp. 4485–4487, 2001.

[73] J. Federici, D. Gary, B. Schulkin, F. Huang, H. Altan, R. Barat, and D. Zimdars, "Terahertz imaging using an interferometric array," *Appl. Phys. Lett.*, vol. 83, pp. 2477–2479, 2003.

[74] T. Dorney, W. W. Symes, and R. G. Baraniuk, and D. Mittleman, "Terahertz multistatic reflection imaging," *J. Opt. Soc. Amer. A*, vol. 19, pp. 1432–1442, 2002.

[75] T. S. Hartwick, D. T. Hodges, D. H. Barker, and F. B. Foote, "Far infrared imagery," *Appl. Opt.*, vol. 15, pp. 1919–1922, 1976.

[76] N. Karpowicz, H. Zhong, C. Zhang, K.-I. Lin, J.-S. Hwang, J. Xu, and X.-C. Zhang, "Compact continuous-wave subterahertz system for inspection applications," *Appl. Phys. Lett.*, vol. 86, p. 054 105, 2005.

[77] A. Dobroiu, M. Yamashita, Y. N. Ohshima, Y. Morita, C. Otani, and K. Kawase, "Terahertz imaging system based on a backward-wave oscillator," *Appl. Opt.*, vol. 43, pp. 5637–5646, 2004.

[78] J. Darmo, V. Tamosiunas, G. Fasching, J. Kröll, K. Unterrainer, M. Beck, M. Giovannini, J. Faist, C. Kremser, and P. Debbage, "Imaging with a Terahertz quantum cascade laser," *Opt. Express*, vol. 12, pp. 1879–1884, 2004.

[79] K. Siebert, H. Quast, R. Leonhardt, T. Löffler, M. Thomson, T. Bauer, and H. G. Roskos, "Continuous-wave all-optoelectronic terahertz imaging," *Appl. Phys. Lett.*, vol. 80, pp. 3003–3005, 2002.

## ABOUT THE AUTHORS

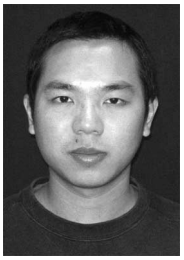

**Hai-Bo Liu** (Member, IEEE) was born in Guilin, China, in 1975. He received the B.S. degree in chemical physics from the East China University of Science and Technology, Shanghai, China, in 1997, the M. S. degree in optics from the Fudan University, Shanghai, China, in 2000, and the Ph.D. degree from the Department of Physics at Rensselaer Polytechnic Institute, Troy, NY, in 2006. His doctoral research involved terahertz spectroscopy for chemical and biological sensing applications.

After graduation, he joined InterScience Inc., Troy, as a Research Scientist. His research interests include sensing explosives and related compounds with both pulsed and continuous-wave terahertz technologies, and using terahertz spectroscopy to study biological cells, pharmaceutical materials, proteins, and other biomolecules.

Dr. Liu has been a member of the Optical Society America since 2002. During his study at Rensselaer Polytechnic Institute, he received the Coherent Award in 2004, the Harry F. Meiners Fellowship in 2002, and the Walter Eppenstein Award in 2002.

**Hua Zhong** received the B.S. degree in physics from Peking University, Beijing, China in 2000 and the M.S. and Ph.D. degrees in physics from Rensselaer Polytechnic Institute, Troy, NY, in 2002 and 2006, respectively.

Her research interest is nondestructive evaluation, and standoff distance sensing and imaging with both pulsed and continuous-wave terahertz radiation.

**Nicholas Karpowicz** received the B.S. degree in physics and philosophy from the Rensselaer Polytechnic Institute, Troy, NY, in 2003. He is currently working toward the Ph.D. degree in the Department of Physics, Rensselaer Polytechnic Institute.

He is a National Science Foundation IGERT Fellow in Terahertz Science and Technology at Rensselaer Polytechnic Institute. He has participated in research mainly on imaging with pulsed and continuous-wave THz radiation and on THz imaging in both near-field and far-field regimes. is currently working on functional, far-field imaging with THz pulses.

**Yunqing Chen** received the M.S. degree in physical chemistry from Northwestern University, Xi'an, China, in 1990 and the Ph.D. degree in physical chemistry in the Institute of Chemistry, Chinese Academy of Sciences, Beijing, in 1999.

In 1999, he was a Postdoctoral Associate at Wadsworth Center, New York State Department of Health, Albany. In 2003, he jointed Rensselaer Polytechnic Institute, Troy, NY, as a Research Associate. His current involvement is mainly with Terahertz spectroscopy.

Dr. Chen has been a member of the American Chemistry Society since 2000.

**Xi-Cheng Zhang** (Fellow, IEEE) received the B.S. in physics from Peking University, Beijing, China, in 1982 and the M.Sc. and Ph.D. degrees in physics from Brown University, Providence, RI, in 1983 and 1986, respectively.

He was a Visiting Scientist at the Massachusetts Institute of Technology in 1985. From 1985 to 1987, he worked in the Physical Technology Division of the Amoco Research Center. From 1987 to 1991, he was in the Electrical Engineering Department at Columbia University. He then joined the Rensselaer Polytechnic Institute in Troy, NY, where he has been a faculty member since 1992. He is currently the J. Erik Jonsson Professor of Science, a Professor of Physics, Applied Physics and Astronomy, and a Professor of Electrical, Computer, and Systems Engineering at Rensselaer Polytechnic Institute. He is the founding director of the Center for Terahertz Research at Rensselaer. He has authored and coauthored eight books and book chapters and more than 250 refereed journal papers. He has participated in over 300 colloquium, seminars, invited conference presentations, and 250 contributed conference talks since 1990.

Dr. Zhang is a fellow of the American Physics Society and the Optical Society of America.